THE BELL SYSTEM TECHNICAL JOURNAL
Vol. 50, No. 9, November, 1971
Printed in U.S.A.

A Microwave Feed-Forward Experiment

By H. SEIDEL

(Manuscript received April 12, 1971)

Both one- and two-stage feed-forward control were applied to a 4-GHz, 461A, traveling-wave tube, used in the TD-3 radio relay system, to demonstrate the feasibility of reducing distortion to a sufficiently low level for single sideband transmission. With a single stage, and discounting extraneous losses, the third-order, M3, distortion measure was reduced by 38 dB over a selected 20-MHz channel, and the application of the second stage rendered distortion unobservable with our instruments. These results were time independent with continuous performance over several months.

I. INTRODUCTION

This paper describes an experimental microwave amplifier, designed around the Western Electric 461A traveling-wave tube, which operates with extremely low modulation products over a 20-MHz-wide microwave radio channel. The experimental results provide a fair assurance of the capability of such amplifiers for field use, with a prospect of significantly increasing the channel capacity of microwave radio systems by permitting the use of single sideband AM rather than FM transmission.

This work is part of a continuing effort to explore and exploit feed-forward error control techniques. Feed-forward error control was originated by Harold S. Black in 1924,[1] a precursor by several years to his more famous accomplishment of feedback control. Through 1960, it was viewed, somewhat, as a curiosity,[2] and was used only in the context of a McMillan circuit[3] which fused the two Black concepts of feedback and feed-forward.

Of interest in view of the present publication is U. S. Patent 2,592,716 issued in 1952 to W. D. Lewis, who extended McMillan's ideas to microwaves using traveling-wave tubes and other microwave hardware, to yield redundancy. As proposed, there are fundamental differences

to the results presented here, primarily with respect to unequal amplifier division, and the explicit equalization of signal path timing. Nevertheless, the failure of his ideas to achieve greater currency, leading ultimately to developments parallel to those presented here, probably reflects only to the difference of pressures spanning twenty years.

The essential feature of feed-forward is its total freedom from transit time limitations which seriously limit the application of negative feedback at high frequencies. H. Seidel, H. R. Beurrier, and A. N. Friedman,[4] in 1967, demonstrated the capabilities of feed-forward when applied to VHF amplifiers. Two separate high-power amplifiers, one operating between 25 and 35 MHz and the other between 60 and 90 MHz, were made to exceed dynamic ranges of well over 100 dB, using circuit features adapted to the requirements of feed-forward error control.

In 1969, the author demonstrated the capabilities of feed-forward control in improving an existing L-4 coaxial cable distribution amplifier. This amplifier, at the forefront of 1966 transistor and feedback art, yielded a 40-dB improvement of modulation products across the entire range of 0.5 to 20 MHz,[5] a 40:1 bandwidth. At this juncture, the cumulative evidence made clear the worth and tractability of feed-forward control, and interest arose in its applicability to microwaves.

Of particular interest in microwaves is the distortion of the power output stage of a radio relay repeater. It is well known that amplitude compression forces a frequency modulation, or PCM, or still other frequency redundant modulation schemes, to override the cross-modulation that would be otherwise produced. Redundant frequency solutions may, however, prove ultimately self-defeating. Spectrum width is not readily acquired in a climate of ever-accelerating communication traffic.

Under these circumstances, single sideband modulation is an attractive prospect assuming that, indeed, it is only the power stage limitation that excludes it. For example, the effect of atmospheric fluctuations on wideband single sideband transmission is, as yet, unevaluated, both with respect to fading and scintillation. Nevertheless, if one assumes the dominant limitation to be power stage compression and, assuming generally acceptable noise levels, talker statistics, path losses, etc., together with an assumption of 3600 circuits within a 20-MHz channel, linearity requirements for the power stage may be deduced. For the Western Electric 461A traveling-wave tube, the 10-watt saturation power stage used in the TD-3 system, calculation shows a required improvement in modulation products of between

40 and 47 dB.[6,7] The divergence in these numbers stems from the degree of phase decorrelation introduced into third-order intermodulation accumulation by transposing (frogging) master groups at various sites along the transmission route. To show the adequacy of feed-forward control independent of auxiliary techniques, it was the purpose of this experiment to show that distortion reduction could be accomplished beyond the higher, 47 dB, figure.

To make the linearity requirements precisely quantitative, let us momentarily review the definition of the intermodulation measure, M3. M3 is defined as the number of decibels relative to one milliwatt at which one will find a third-order product of the form A + B − C, with the amplifier emitting the three tones, A, B, and C, each at one milliwatt.[8] The 461A traveling-wave tube has an M3 rating of −78 dB, so that a 47-dB improvement corresponds to an M3 value of −125 dB.

Further specification on the experiment was that each tone in the third-order intermodulation test was to be set to a 22-dBm output power, and that the overall system was not to saturate fully below 38 dBm. Implicit in the specification of 22 dBm per tone is the recognition that third-order intermodulation products would be 3 × 22, or 66 dB, above the −125-dBm level. Therefore, it was the objective of this test to reduce third-order intermodulation below −59 dBm with the specified three-tone excitation. A final specification required that the noise figure not be substantially increased from the present 461A value: a quantity of, roughly, 30 dB.

As we shall show, the various amplifier objectives have been met. There is a current study of atmospheric effects upon single sideband transmission. The combined results of the atmospheric study and the evaluation of the role of low-distortion amplifiers will form a basis for the determination of feasibility of single sideband transmission in microwave radio relay repeaters.

The body of this paper is contained in the following three sections. In Section II the essentials of feed-forward control are reviewed. While, in many respects, it repeats information contained in Refs. 4 and 5, it does contain new information in the form of a noise analysis of a feed-forward system. Embodiment of a feed-forward system is highly influenced by noise considerations and a full understanding of the noise process is important.

Feasibility of a microwave feed-forward amplifier requires, essentially, a demonstration of compatible co-existence of various microwave devices interacting in a fairly complex pattern. The very existence of individual devices capable of satisfying their requisite functions

must be investigated, and then their interaction must be shown to be predictable. While we attempt to separate Device Choices and Experimental Results in Sections III and IV, we cannot claim a fully successful separation. The choice of a device is, in the last analysis, an operational procedure in that its choice must make the total system operate acceptably, and this can only be done, convergently, in evaluating end results as part of the process of device choice.

Section V summarizes the various results of the study and suggests, possibly, profitable areas for further investigation.

II. SHORT REVIEW OF FEED-FORWARD ERROR CONTROL

2.1 *General Features*

Feed-forward control, as we use it, has two major characteristics:

(*i*) It recognizes time flow and provides appropriately adapted control circuitry.

(*ii*) Error is determined relative to the source within each successive stage of growth, thereby not allowing any cumulative increase of error. To the contrary, an arbitrarily low error may be achieved with an ever-increasing number of stages.

Feedback, in comparing input with output, glosses over the fundamental distinction that input and output are not simultaneous events and, therefore, not truly capable of direct comparison. In practice, they are substantially simultaneous if device speed is far faster than the intelligence rate into the system. Device speed enters the problem, therefore, not in a fundamental sense, but only as a means of making the operational procedure of feedback acceptable. If we were to organize a system of error control which did not force a false requirement of simultaneity, not only would the problem of fabricating zero transit time devices disappear, but so would the entire problem of stability, another guise of the consequence of comparing incomparable events.

Using the first feature listed for feed-forward, we recognize the character of transit time in forming a proper error function. Rather than compare input with output, we form a delayed reference of the input, where the time delay employed sets a standard for the transit time of the amplifier. We assume that the amplifier deviates from this time value to only a small degree. Comparison of the output with the delayed input is made through a sampling coupler whose coupling loss is nominally the gain of the amplifier. Interfering the sampled amplifier output with the delayed reference, we form an error referred in time to the amplifier output.

In having both the amplifier output and the error component of the output in a frame properly referred to the source, we have an undegraded system. Thermodynamically there is no disorder added to the system by the amplifier since the error function provides the means to separate out what is desirable and what is undesirable in the amplifier output. This includes amplifier distortion, undesired variation in the transfer function, and thermal noise. In the sense of Brillouin,[9] the input signal information constitutes a "negative entropy" and we may employ it to cool the noise temperature of the amplifier. As indicated in the second feature of feed-forward, irrespective of complexity as the system grows, we may touch back again and again to this negative entropy to keep the system as cool in noise temperature as we may wish.

Having determined error, the next step in the process is to remove the error present in the amplified output. The process is, essentially, one of subtraction, implemented through a time compatible interference means. The detected error is amplified and brought back to the original error level in the amplifier output. During the transit period of amplification, both the signal and error in the amplifier output are appropriately delayed, so that the error of the main amplifier output and the amplified detected error may collide and annihilate in the final combining coupler.

In amplifying the detected error, we do degrade it somewhat in terms of the thermal noise and distortions of the correction amplifier so that error correction is not perfect. Further the annihilation of the original error is imperfect because of small transfer function perturbations within the error cancelling interferometer loop. While much reduced, the residual error is finite and circumstances may require greater reduction. Treating the two loops composing the error reduction stage as an algorithmic process, we may repeat that process arbitrarily by embedding the amplifier at each level of correction in still another two-loop error correcting stage. There is no cumulative error produced by multistaging since we touch back to the original signal, for reference, at each stage.

Two simplified feed-forward error control systems are shown in Fig. 1 following the lines of description given above. Figure 1a shows a single-stage correction system, where the term "stage" implies both an error detecting loop and an error cancelling injection loop. In this figure, we abstract the common phases produced by respectively equal time delays. The main amplifier is characterized by a small, relative complex error, δ. The auxiliary amplifier, referred to at times as the subsidiary amplifier, or the correction amplifier, is characterized by

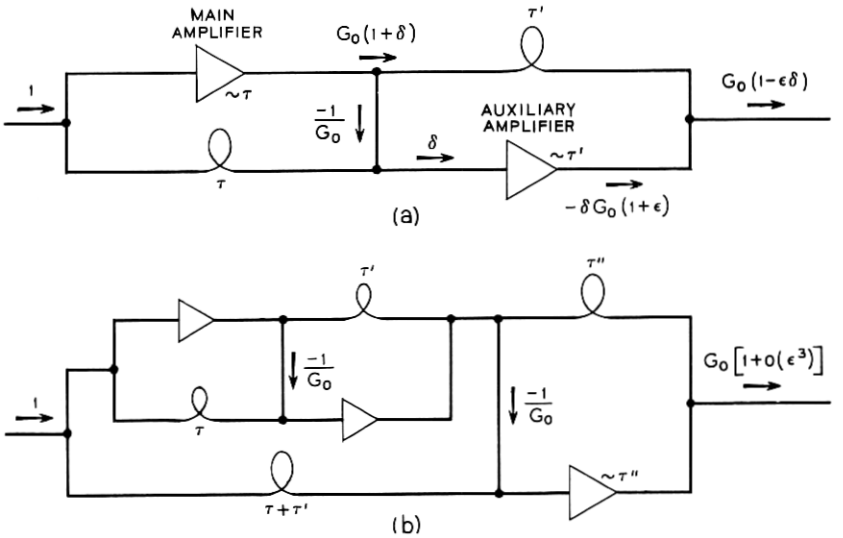

Fig. 1—Feed-forward error control systems: (a) single stage; (b) double stage.

a relative error ϵ. Both of these quantities are small and we find the output to have an error of second-order smallness, equal, relatively, to $\delta\epsilon$.

Figure 1b shows a two-stage correction system in which the entire first stage is embedded in a second stage for another two-loop cycle of correction. The second-order error of the original single-stage amplifier is now rendered by the second stage into a third-order error through an identical iteration of the mechanics of the error cancellation circuit.

2.2 *Thermal Noise*

In its use here as a power stage output amplifier, thermal noise requirements on the amplifier are modest since it is driven at high level. Nevertheless, without appropriate caution, thermal noise could, inadvertently, become a major problem in a multistage feed-forward system. The crux of the matter lies in the specific means by which we extract information from the original source. If sampling at each correction stage depletes signal energy availability, signal-to-noise level reduces and the reference loses its quality as an information source. To understand the thermal noise aspects, let us calculate the observed noise system with ideal error cancellation.

A feed-forward correction stage is shown in Fig. 2 with noise sources

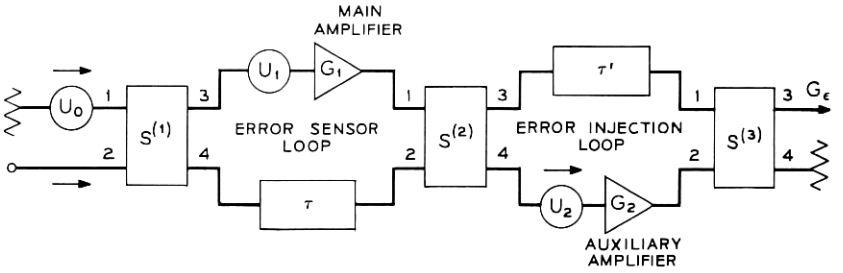

Fig. 2—Feed-forward stage with included noise sources.

included. The uncorrelated noise sources U_o , U_1 , and U_2 represent the incident portions of the noise waves, respectively, of the matched termination of the input coupler $S^{(1)}$, the referred input noise of the main amplifier, and the referred input noise of the auxiliary amplifier.

If we assume ideal operation of both interferometer loops, we may immediately discount the effect of U_1 since it is headed for ultimate annihilation in the final output. Consequently, we are concerned only with the black-body noise, U_o , and the auxiliary amplifier noise, U_2 . A normalization to black-body emission will be taken in all that follows so that $|\overline{U_o^2}| = 1$. Lack of correlation between U_o and U_2 provides a further condition that Re $(\overline{U_o U_2^*}) = 0$.

Let us abstract time considerations from G_1 , and G_2 in all that follows, since that function is formed by the delay networks τ and τ'. To within these times, the interferometry conditions on the two loops of Fig. 1 are as follows:

$$S_{23}^{(1)} S_{14}^{(2)} G_1 + S_{24}^{(1)} S_{24}^{(2)} = 0, \tag{1}$$

$$S_{14}^{(2)} S_{23}^{(3)} G_2 + S_{13}^{(2)} S_{13}^{(3)} = 0. \tag{2}$$

These two equations permit major simplification in calculation. They assert, implicitly, that either G_1 or G_2 , exclusively, may be disabled without affecting ideal performance. We shall use these disabling features selectively, disabling G_2 for gain calculation and disabling G_1 for noise calculation.

For overall gain, we have,

$$\mathcal{G} = (S_{23}^{(1)} S_{13}^{(2)} G_1 + S_{24}^{(1)} S_{23}^{(2)}) S_{13}^{(3)}. \tag{3}$$

The couplers in Fig. 1 are all directional and forward scattering, having the general description,

$$S = \begin{bmatrix} 0 & 0 & S_{13} & S_{14} \\ 0 & 0 & S_{23} & S_{24} \\ S_{13} & S_{23} & 0 & 0 \\ S_{14} & S_{24} & 0 & 0 \end{bmatrix}. \tag{4}$$

Because of their lossless nature they satisfy the further condition that unitarity applies and

$$(S^T)^* S = 1. \tag{5}$$

Using (1), (4), and (5) in conjunction with (3), we obtain

$$\mathcal{G} = \frac{S_{24}^{(1)} S_{13}^{(3)}}{S_{23}^{(2)*}}, \tag{6}$$

where calculation details are shown in the Appendix. The noise output is given by

$$\epsilon = \{U_o[S_{14}^{(1)} S_{24}^{(2)}] + U_2\} G_2 S_{23}^{(3)} + U_o S_{14}^{(1)} S_{23}^{(2)} S_{13}^{(3)}. \tag{7}$$

Again using calculational details shown in the Appendix, we find

$$\epsilon = \frac{S_{13}^{(3)}}{S_{23}^{(2)*}} (U_o S_{14}^{(1)} + U_2 S_{24}^{(2)*}). \tag{8}$$

The relative noise temperature, T, of the feed-forward amplifier is given by†

$$T \equiv \frac{|\overline{\epsilon^2}|}{|\mathcal{G}|^2},$$

and the relative noise temperature of the auxiliary amplifier is $T_2 \equiv |\overline{u_2^2}|$. From (8), after minor transformation,

$$T = \frac{|S_{14}^{(1)}|^2 + T_2 |S_{13}^{(2)}|^2}{|S_{13}^{(1)}|^2}, \tag{9}$$

where the recognition is made that $|S_{24}^{(m)}|^2 = |S_{13}^{(m)}|^2$. A further relationship, easily deduced from (1) and (6), is

$$\frac{|G_1|^2}{|\mathcal{G}|^2} = \frac{1}{|S_{14}^{(1)}|^2} \frac{|S_{13}^{(2)}|^4}{|S_{13}^{(3)}|^2}. \tag{10}$$

The full noise design problem may be understood as a reconciliation between (9) and (10). We cannot afford to lose too much of the main

† The relative noise temperature, T, of the amplifier is defined such that the output noise contributed by the amplifier is 290 kTBG, where k is Boltzmann's constant given in joules/°C.

amplifier output so that $|S_{13}^{(2)}|$ and $|S_{13}^{(3)}|$ must be quantities close to unity. Equation (10) states that a small value of $|S_{14}^{(1)}|$ infers the need of a large main amplifier gain, G_1, to yield a specified system gain $\mathcal{G}$. If, however, $|S_{14}^{(1)}|$ were made too large, $|S_{13}^{(1)}|$ would reduce, correspondingly, since these two matrix elements share the complete power flow of the coupler. Any significant reduction of $|S_{13}^{(1)}|$ raises the noise temperature of the system, by virtue of (9), so that its value must be guarded.

The noise reconciliation with excessively large main amplifier gain requirements is as follows. Main amplifier noise does not enter into the final system noise temperature in principle, for an ideal error cancelling system. This holds in practice, as well, providing main amplifier noise is not allowed to achieve that level which can compete with the degree of cancellation in the last stage. In constructing a multistage system, therefore, we would allow the order of 6 dB noise increase per stage by making $|S_{13}^{(1)}|^2$ correspond to about -6 dB, up until the last stage, losing about 1 dB gain per stage in the process. For the last stage, treating all previous stages as a new, noisy, main amplifier, we reverse the process, causing the final system noise temperature to exceed that of the last auxiliary amplifier by about 1 dB, but losing 6 dB of gain.

Equation (9) permits a simple, useful approximation. Typically, $|S_{13}^{(2)}|^2$ deviates by less than 1 percent from unity and $|S_{14}^{(1)}|^2$ is well less than unity. T_2, on the other hand, may range anywhere from a value of 3 or 4 in a practical system to well beyond 1000. A good approximation for (9) is

$$T = \frac{T_2}{|S_{13}^{(1)}|^2}, \tag{11}$$

which states that the noise temperature of a well-cancelled feed-forward system is given by the noise temperature of the final auxiliary amplifier times the transmission loss to the reference path produced by the reference coupler.

2.3 *Criteria for Interferometer Balance*

Each stage of correction requires two interferometer balances. The first, corresponding to (1), sets the standards for phase and gain of the main amplifier, while the second, corresponding to (2), cancels the imbalance products proceeding from the first. Nominally, the first loop comparison coupler and time delay closely approximates the transfer properties of the main amplifier, so that the error signal

due to small transfer function perturbation is small. If the standards of coupling loss and time delay were in small error, the system would operate to slightly different standards, with little consequence other than a somewhat higher average power operation of the auxiliary amplifier.

Alternatively, intermodulation and thermal noise are relatively incoherent with respect to the reference signal, so that they form imbalance products of the first interferometer loop independent of the precision of its balance with respect to the coherent portion of the signal. It is the second interferometer loop balance which is critical in cancelling these products from the output.

The relative precisions of the two interferometry relations, (1) and (2), are to be viewed from entirely different perspectives in system design. Given moderate dynamic range of the final auxiliary amplifier, the first loop must only possess that degree of cancellation to avoid any substantial manifestations of nonlinearity in the auxiliary amplifier. On the other hand, the entire figure of merit of the feed-forward error control system in yielding linearity improvement resides in the precision of balance of the second interferometer loop. Since this loop operates in relatively lightly loaded fashion, the potential for maintaining precise balance is good. As we shall show, major design effort is expended towards maintaining a time-independent excellence of this balance through the use of auxiliary controls.

III. DEVICE CHOICES

3.1 *First-Stage Devices*

Within a feed-forward microwave system we must seek acceptable choices of microwave amplifier, means of accommodating relatively large time delays, couplers adapted to the needs of precision interferometry, adjustment means for setup, adaptive controllers to maintain time-independent operation, etc. The adjective "acceptable" suggests not only the use of devices capable of meeting strictly technical objectives, but implies objectives, as well, of ultimate reproducibility, economic manufacture, and compact packaging.

While, in the longer term, one would think of microwave integration of many of the components used in the amplifier system, such integration is incompatible with the immediate needs of a feasibility demonstration. The microwave experiment, therefore, was performed entirely with waveguide and coaxial circuitry to provide for ease of modification. In general, a one-to-one correspondence exists between most of these

components and what exists within the present art of microwave integrated circuitry. Nevertheless, two devices would appear to except themselves, at this juncture, from realization within integrated format. They are:

(*i*) main power amplifier, and

(*ii*) error cancellation time delay section.

The main amplifier used in the experiment is a 461A traveling-wave tube capable of the order of 10 watts of saturated power at 4 GHz. While one may envision an ultimate solid-state replacement, such replacement is not now available. The time delay miniaturization problem is even less tractable than that of the main amplifier. The error cancellation time delay section, shown as τ' in Fig. 1a, offsets the 13-ns transit time of the auxiliary amplifier, another 461A TWT. At 4 GHz this transit time corresponds to 52 cycles of storage, and the storage loss is absorbed from the output power of the main amplifier. Since the economics of generating distortion-free power is severe, it would seem unlikely that one would elect to waste that power through the use of a relatively lossy miniaturized delay line.

3.1.1 *Main Amplifier*

Two devices contended for the role of the main power amplifier: the 461A TWT used in the TD-3 system, and the 416C closed-spaced triode used in the transmitter amplifier in the TD-2 system. The 461A TWT was selected because of its superior gain and phase stability. In contrast to a transit-time-limited system the intrinsic functions of a traveling-wave tube (i.e., beam formation, drift, interaction, beam collection) are all well separated. While transit time may be large, nevertheless it is well characterized by a highly regulated helix potential as well as by the precision of the helix construction itself. Thermal heating of the helix through beam interception is imperceptible and its electrical phase is well maintained in a controlled ambient environment. Given a control of cathode current and a maintenance of beam synchronism, no significant aging problems appear evident. While some effect may be postulated of the accumulation of ionized gas molecules within the beam, estimations yield minor gain and phase level shifts, with no appreciable effect on time delay.

An attempt to grossly simulate TWT aging has been made varying beam-forming electrode potentials. While minor shifts were observed in gain and phase levels, these shifts were well within the corrective range of automatic controllers which we shall describe later. The essential result of this investigation is that transit time is unaffected

and that fixed feed-forward delay compensations retain their performance with time.

Measured performance over a 100-day period tends to support the favorable view of TWT capability. Figure 3 shows gain fluctuations of the order of ±0.05 dB after a two-day stabilization period. The phase data of Fig. 4 show a stabilization period of, perhaps, ten days, followed by a drift of average phase of 1 degree in the remainder of the 100-day period. Short-term phase fluctuations appear to be within ±0.25 degree.

To place these fluctuations within context, a 40-dB interferometer null implies either a gain imbalance of 0.08 dB or a phase imbalance of 0.6 degree, or a weighted combination of both. The small open-cycle fluctuations of the TWT lend themselves readily to active control means to provide for interferometer balance well beyond the 40-dB level.

3.1.2 *Subsidiary Amplifier-First Stage*

The subsidiary amplifier employed in the first stage was another 461A TWT. The determining factor in its choice was, primarily, that it was a standard device already employed in the Bell System, although its power capacity exceeded the needs of the experiment.

It is instructive, nevertheless, to consider the requirements on the first-stage subsidiary amplifier in the light of the M3 specifications for the entire feed-forward amplifier system. Relative to its own M3

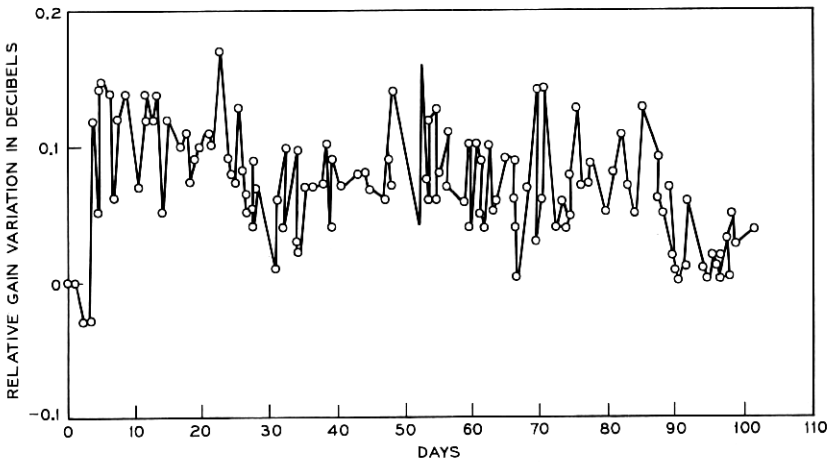

Fig. 3—Gain variation for 461A TWT amplifier.

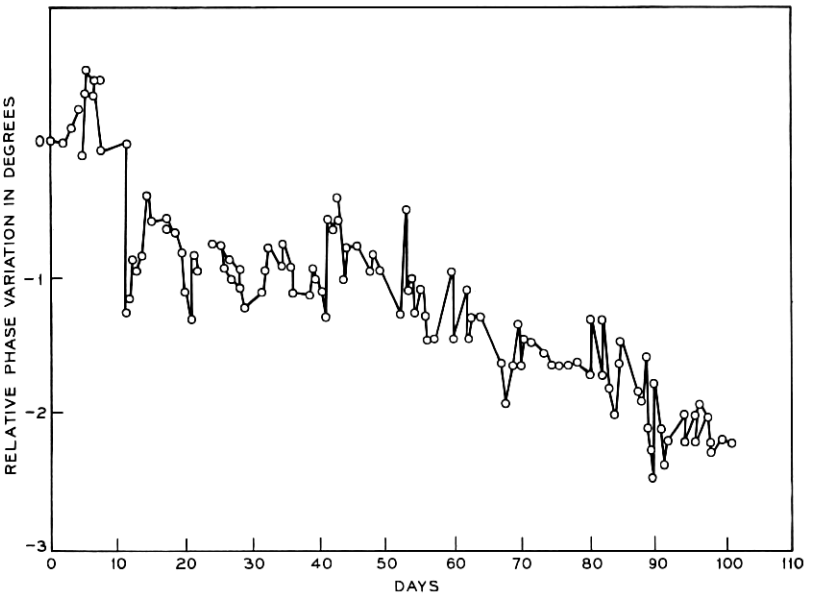

Fig. 4—Phase variation for 461A TWT amplifier.

rating of −78 dB, the main amplifier produces third-order intermodulation tones of −12 dBm for the three specified 22-dBm output tones. Thus, intermodulation tones are of order 34 dB below the main signal tones. If these tones form the substantial level of excitation into a subsidiary amplifier of capacity identical to the main amplifier, the new production of intermodulation would lie at about −96 dBm taking into account the 6-dB transfer loss in the error combiner coupler.

The desired intermodulation level for the feed-forward system for 22 dBm/tone output is −59 dBm, so that a margin exists of 37 dB. If we assume a first-stage reference loop imbalance of order 35 dB, the subsidiary amplifier must also handle this energy as if it were error. Such imbalance error is, roughly, at the same level as the intermodulation and diminishes the margin. Recognizing the three-for-one relation of intermodulation production, in dB, to power capacity, one might envision a new code of manufacture for the first-stage subsidiary amplifier designed to meet all the specifications as given having only 10 percent the capacity of the 461A.†

† Since the initial specifications were given, more recent requirements have stipulated an M3 of −125 dB to the peak 38-dBm level. Calculation shows that this more demanding performance could still be handled by a subsidiary 461A TWT, but at 100 percent of its capacity.

However, even within these specifications, this degree of capacity reduction may be somewhat optimistic. Unlike a conventional amplifier, a singly corrected feed-forward system increases in intermodulation at a rate of 9 dB per dB with subsidiary amplifier saturation, and at a rate of 27 dB per dB for a doubly corrected system. Such precipitous distortion increase would suggest greater caution in establishing power margins.

3.1.3 *Delay Lines*

Both the error sensor loop and the error injector loop of the first stage house 461A traveling-wave tubes, each about 19,000 degrees in electrical length. Corresponding to each loop is an equivalent delay line designed to match its respective traveling-wave tube to within a precision of better than 1/2 degree.

By excellent helix design and construction techniques, phase distortion is maintained at minimal levels in the traveling-wave tube, and phase linearity is achievable within the level of precision sought. The onus falls on the matched delay section within each interferometer loop to match that degree of excellence. A problem arises of sheer bulk. The helix produces large attenuation because of its small cross section relative to physical length, but this is inconsequential because of electronic gain. There is no gain mechanism, however, in the sensor loop delay line, nor in the injector loop delay line. Large attenuation in the former increases system noise figure by that amount, whereas, attenuation in the latter dissipates expensively bought power.

There are some options on noise performance since we are discussing a high-level amplifier, and this should merit further investigation. We might accept some tolerably higher level of noise figure and allow a degree of compromise in miniaturizing the error sensor loop delay line. As stated, however, an excessively dissipative error cancellation delay line is unacceptable, since that line directly tandems the main power amplifier. Consequently, at least the error cancellation delay line is composed of standard cross-section waveguide. Having accepted the necessity for one large section delay line, for convenience, we made the second, corresponding to the error sensor loop, exactly similar.

With hardware pertinent to the system added, the actual time delay within each loop exceeds 15.5 ns. Using straight WR229 waveguide, this calls for a span of 11.93 feet for each delay line section. This length proves awkward to package, particularly with the knowledge that it must be used repeatedly within the feed-forward assembly.

The simultaneous need to retain waveguide cross section and to

make packaging practical suggests use of filter techniques to increase energy storage per unit length. Since the filter must not ripple or bow the phase linearity in any substantial manner, nor be permitted to distort the amplitude response substantially, we chose a moderately wide bandwidth, maximally flat, filter as a basis for design. Computation shows that one may realize the delay section to within 0.0002 dB amplitude and 0.1 degree phase ripples over the 20-MHz band with a 14-inch, six-section, asymmetric inductive iris, direct-coupled filter. The computation does not account for iris thickness, and physical realization with 1/32-inch-thick irises shows excellent preservation of relative shape of characteristics but modifies time delay by a small factor. As a practical matter, the time delay computed is designed at 15 percent lower than that required. This empirical determination has been found operational over a significant span of time delay. Residual errors are simply tailored by the addition of a small guide length so that accurate time control is easily achieved within a relatively compact package.

3.1.4 *Directional Couplers*

Control of amplitude is the counterpart to the control of time delay in a broadband interferometer loop. Since amplitude levels are set, primarily, by directional coupling ratios in the feed-forward system's interferometer loops, one need only require flat coupler over a negligible 1/2-percent bandwidth. Given a fixed design ready for manufacture, such couplers are easily obtained. However, in the case of an experimental system requiring close, adjustable, control, it is impossible to think of a continuum of couplers made conveniently available.

Fortunately an adjustable directional coupler is readily available—but at a price. In essence, the coupler is composed of two circulators with an adjustable cutoff section intervening, and is shown in Fig. 5. The price to be paid is the dissipation of two passes through the circulator plus the small dissipation in reflecting from the cutoff section. These losses form part of the excess loss picture to which we shall refer later, but which would not be present in a final design.

In Fig. 5, wave energy incident upon port A impinges entirely upon the mismatch section in the first pass through the circulator. Most of that energy reflects via circulation to port B. That energy transmitted through the cutoff section circulates to port C. Energy reflected from B returns only to A and, similarly, all reflection from C returns only to D. The coupling ratio of this coupler system is, substantially, the insertion loss of the cutoff section which, as indicated, is controllable.

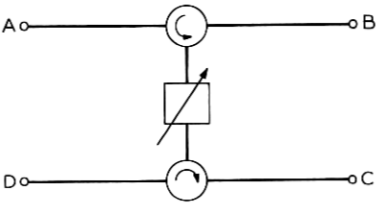

Fig. 5—Adjustable directional coupler.

As used throughout, the controllable cutoff section, shown in Fig. 6a, is composed of two inductive irises forming an off-resonance cavity, and three symmetrically located screws spanning 1/4 λ_g of length of this cavity.

Scattering matrix properties of a reactive, reciprocal, symmetric two-port readily yield a phase quadrature relationship between the reflection and transmission coefficients. Since two passes through equivalent circulators is required to go from A to either B or C in Fig. 5, the 90-degree phase difference between these two ports is unaltered by symmetric adjustment of the cutoff section. Therefore, phase and gain adjustments of the interferometry conditions are entirely independent.

The two irises of the cavity are spaced essentially to be at a peak of the first rejection region, as shown in Fig. 6b, where the iris susceptance value defines a particular loss. Simultaneous motion of the two outer screws, without the presence of the center one, controls internal phase within the cavity. This tends to change the center frequency corresponding to peak loss, with only a minor interaction with that loss. The center screw operating by itself produces a dominant shift of peak loss, with only a minor interaction with center frequency. With both sets of controls operating, various intermediate control relations are obtained. Thus, control of amplitude and flatness is simply afforded without phase interaction.

3.1.5 *Adaptive Control*

The 461A traveling-wave tube has two types of drift, both slow but of widely differing time periods. There is a "breathing" effect which produces 1 degree and 0.1 dB changes throughout a day, probably attributable to thermal effects, and there is a larger term aging process which changes phase by 2 degrees and gain by 0.1 dB over a 100-day period. While these changes are not profound, they exceed the bounds set for the degree of interferometer balance sought. For continuous

operation of the system at target specifications an adaptive control system must be employed to maintain initial balance.

The phase and gain drift variations are nondispersive. For example, a 2-degree drift represents a microscopic change of transit time considering a total electrical length of 19,000 degrees. A simple phase shifter, having in itself a negligible transit time, suffices to compensate this drift across an entire 20-MHz band with fully adequate precision. Precisely the same consideration holds for gain drift control.

To set a test for balance, a continuous pilot tone is injected into the system at a position following the main amplifier in the manner shown in Fig. 7 (point 1). By hypothesis, since this signal appears as an uncorrelated emission of the main amplifier, the feed-forward system must operate to remove it through the interferometric cancellation of the error injector loop.

The quality of interferometric null can, of course, be observed at the output of the first stage, and a performance measure may be made. Unfortunately, it is difficult to discern within the degree of balance accomplished by the interferometer a quantitative evaluation of how much was attributable to phase and how much to gain in failing to achieve a more perfect balance. One may propose a variety of systems to achieve this determination, such as one operating by successively rocking phase and gain to achieve a deepest null. Several possibilities were considered, but we felt them to be more elaborate than the system finally used.

Assuming that the transfer characteristics of the final coupler in which the two paths destructively interfere are highly stable, we may measure the differential gain and phase, respectively, of the two paths

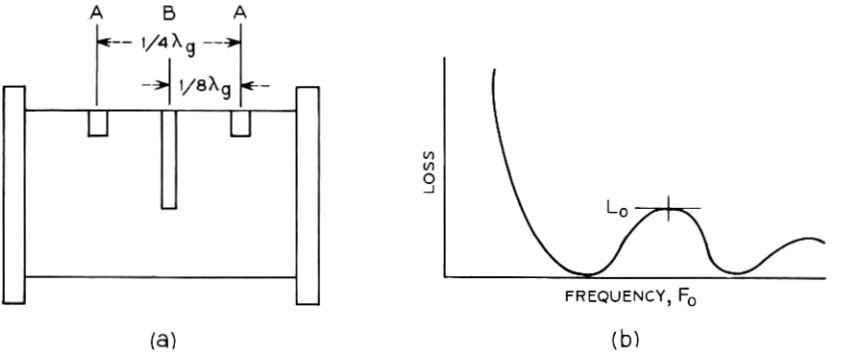

Fig. 6—Controllable cutoff section.

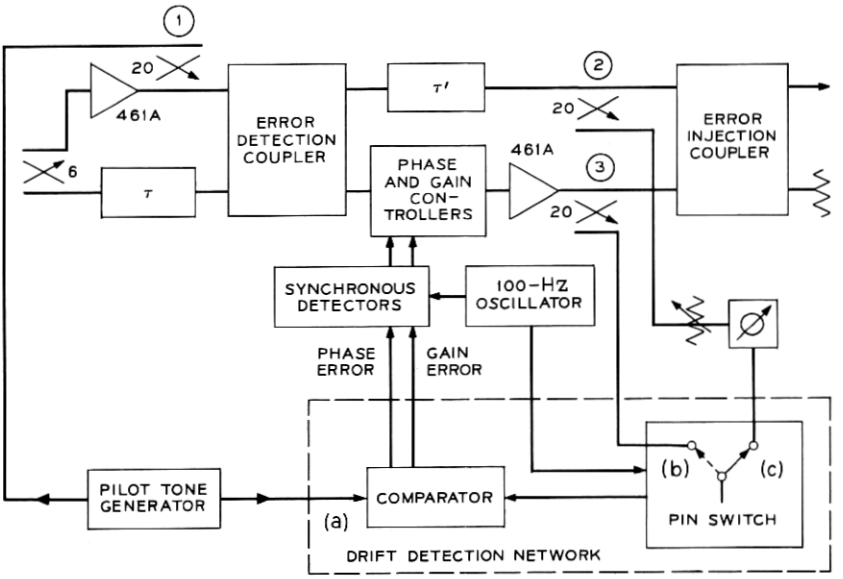

Fig. 7—Drift control in first stage.

prior to interference, and servomechanically correct those differential quantities relative to standards known to yield best destructive interference. Operating in this manner, we have recognized the relative identity of each path within the interferometer and are not confronted with an admixed relationship of these two paths, as we would be in testing the final null.

The two paths of the error injector loop are sampled, via directional couplers, at points 2 and 3 in Fig. 7. These two samplings are brought to points labeled *b* and *c* in the Drift Detector, while the original pilot tone reference connects at point *a*. Intervening in one of the sampled paths is an adjustably set attenuator, phase shifter combination.

The detection of drift is accomplished through means reminiscent of a Dicke radiometer.[10] A known reference to phase is given at point *a*. A switch, synchronously shuttling between *b* and *c* at a 110-Hz rate, samples each of the interferometer paths. By an internal phase discriminator arrangement, it compares the phase of *b* to *a* at one extreme of the switch, while comparing the phase of *c* to *a* at the other. Let the adjustable phase shift control in sampling path *b* be preset such that the output detector readings, corresponding to both *b* and *c*, are identical. With drift, a phase sensitive synchronous signal develops which tags the

direction of the drift and, with synchronous detection, generates a control signal. The attenuation drift detection is accomplished similarly, with the initial set attenuator in path *b* providing a zero amplitude error in the balanced state, and with the phase sensitive synchronous signal tagging the direction of amplitude drift.

The interferometer null drift is, relatively, very slow and the synchronous detection of gain and phase deviation may be made with long correlation times: a fraction of a second or longer. This yields excellent precision in detection, with negligible requirements on pilot tone power for good sensitivity. Given the narrow band nature of this signal, high feedback gain may be employed, and the loop null may be actively restored to limits far exceeding requirements on the feed-forward system.

The controllers employed within the experiment were mechanically driven devices. Electronic phase shift using varactors was ruled out because of the possibility of its generating intermodulation. By default, since an external electronic phase control could not be used, the electronic control of attenuation through a PIN diode was also excluded to avoid noncommon circuitry. Direct electrode control of the TWT was a considered possibility. Tests were made showing that small helix voltage perturbation about synchronous velocity produced phase shift with a negligible attenuation variation. Beam current control affects both phase and amplitude. Using a fast helix voltage feedback and a slow beam current feedback, gain and phase control may be individually achieved. While this may well prove an operational solution in ultimate use, such control meant tampering with a highly regulated power supply during an experiment, and we chose the least adventurous approach.

The mechanical controllers were of similar construction, using a resistive vane in a guillotine attenuator arrangement, and a dielectric vane in like manner for phase shift. To assure no interaction between attenuation and phase control, a shaped dielectric compensation was physically appended to the resistance card to maintain invariant phase with insertion. Each controller, corresponding either to the phase unit or the attenuation unit, was composed of two sections. The first was a manual set to assure initial adjustment, while the second contained a motorized section used in the servomechanical drift adjustment system discussed above. These units are shown in Fig. 8.

The precision of balance is the key to long-term feed-forward microwave error control. The synchronous sampling technique above is excellent for such control, but only if the sampling means is rigorously time independent. A serious question concerns the transmission qualities of the switch.

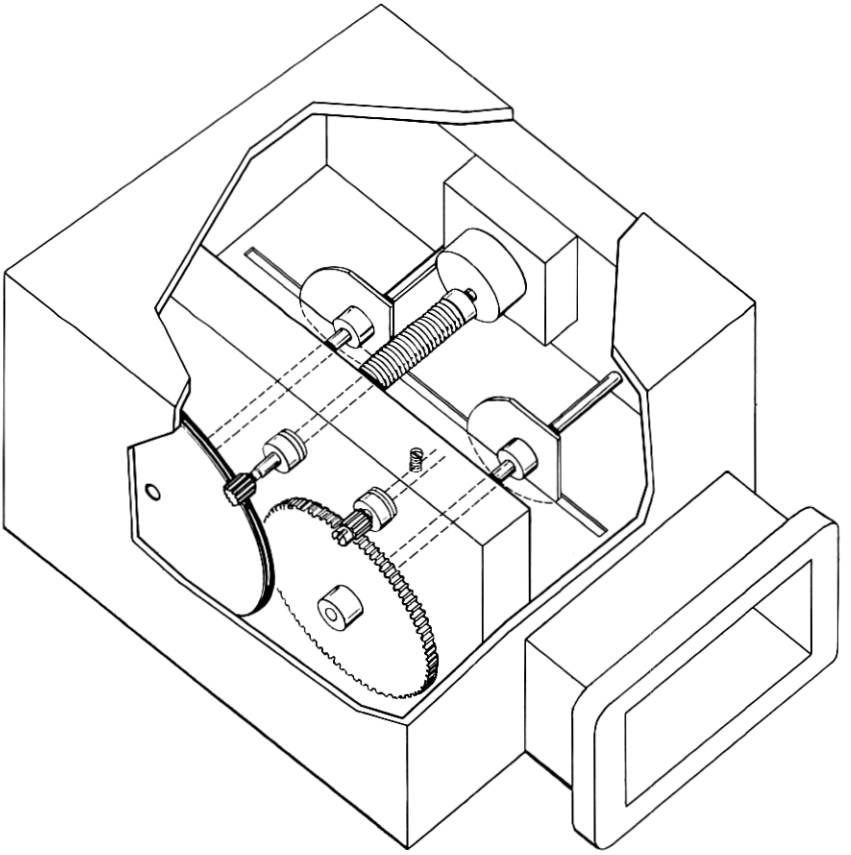

Fig. 8—Mechanical phase/gain controller.

Early in the experiment it was felt that microwave switching might prove complex. Under the circumstance, the sampling signals were individually heterodyned to IF, and all circuitry functions including that of switching were accomplished at IF. This control system worked badly; null balances of the fed-back interferometer loops ranged in time from greater than 50 dB over the band to less than 30 dB. The fault, after intensive examination, was found to lie in the mixers. Over the course of a day, with no overt evidence of thermal gradients between them, and for common fluctuations of local oscillator power and frequency supplied to them, evidence was found of greater than 3 degrees differential transfer phase variation between them in going from micro-

wave to intermediate frequency. The immediate cause of this effect is not understood, but it is probably thermal in origin.

Microwave switching was, thereupon, more rigorously examined and found to be capable of excellent reproducibility. The switch is composed of two oppositely switched sections, each section composed of a shunt PIN diode pair. Each section, individually, lies in the path of one of the sampled signals, and each is followed by an isolator. Both sampling paths are then brought to a common output port using a microwave hybrid combiner. During its transmission cycle, the PIN is strongly reverse biased, but well short of its avalanching. This causes the entire scattering of the diode to reside in its cartridge and to be independent of any semiconductor parameters. In its reflection cycle, the diode is strongly forward biased so that its impedance is dominated by its ohmic contact. Whatever small leakage occurs, at least, does so in a stable manner. The output isolator further stabilizes whatever effect fluctuating impedance might have on the other switching diode pair, although these individual switches are isolated by the conjugacy of the microwave hybrid.

Measurement failed to discern any differential phase or gain shift of the switch although resolvability could be made to within hundredths of a degree and thousandths of a dB. That switching had been the original source of the null softness was confirmed by the very tight system that resulted with the introduction of the PIN switches.

The existence of control circuitry with this caliber of performance was vital to the microwave experiment; without a control capability of this order, a microwave feed-forward system would prove impractical.

3.2 *Second-Stage Devices*

In undertaking this experiment, it was felt that an exploration should be made of the performance of an added second stage with no preconceived concerns as to ultimate system practicability. All the concerns of this section are rendered academic, if only a single stage is to be used. The construction of the second stage was, however, conditioned by the proviso that the first stage be optimally tailored for independent operation, whereas an intent to construct a two-stage system from the start would have led to different choices and, possibly, usages.

3.2.1 *Second-Stage Subsidiary Amplifier*

Most of the elements of the second stage are essentially the same as those of the first, with a major exception being the second-stage subsidiary amplifier. We have recognized in our treatment of the first

subsidiary amplifier that, as a replica of the main amplifier, it possessed greater power capacity than needed. Since the first stage, a composite of these two amplifiers, requires orders of magnitude less correction power, we may properly look to a low-level or weak system for second-stage correction. Indeed, its very weakness is the key to ultimately low noise performance.

The second-stage correction system is shown schematically in Fig. 9. The second-stage subsidiary amplifier is a composite system comprised of a Schottky barrier down-converter, a baseband amplifier, and a varactor upconverter. This combination provides the noise figure of the Schottky barrier, the RF phase and gain stability of the majority carrier Schottky barrier and varactor devices, and the phase and gain stability of a 400-MHz wide baseband amplifier used at a relatively low 70-MHz centerband frequency. This arrangement has the advantage of providing a well-performing solid-state final reference standard to a feed-forward system, operable throughout the microwave spectrum.

The virtue of this arrangement as compared to, say, a microwave transistor amplifier, is clear.

(*i*) Gain per stage is low in a microwave transistor amplifier, and a complex, expensive structure is required

(*ii*) Thermal phase sensitivity is high.

(*iii*) Dynamic range is very low, even for application as a subsidiary amplifier.

(*iv*) General applicability beyond 4 GHz is questionable.

Noise considerations exclude IMPATT and Gunn devices, while

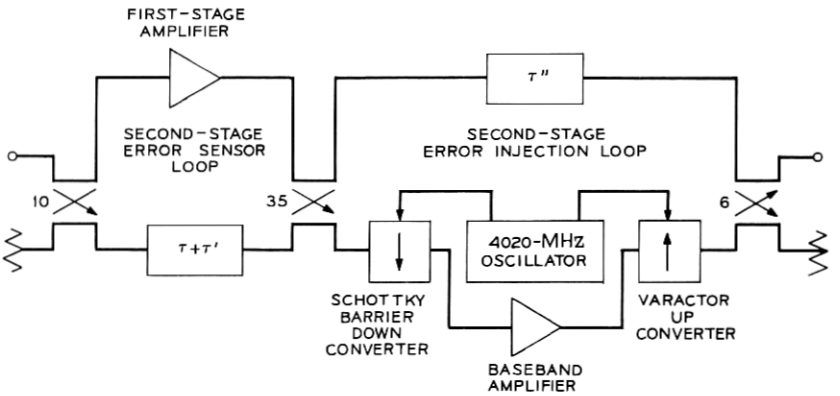

Fig. 9—Second stage.

complexity and/or stability problems make tunnel diode and parametric amplifier systems dubious, for long-term, dependable operation.

In express conflict with our discussion in Section II, Fig. 9 shows the reference arm signal to be dominantly transmitted to the first stage and decoupled by 10 dB from the input, while noise considerations would have it be the other way around. This situation is a direct consequence of the imposed constraint of keeping the first stage intact. Since the first stage was constructed for best noise performance, a substantial loss in gain was incurred in favoring signal into the first subsidiary amplifier. We could not afford to take this loss of gain a second time so that the second stage was run in a high-noise mode. While this rendered noise measurement meaningless, nevertheless, we were able to perform intermodulation measurements with a second-stage correction, and this remains a meaningful measurement irrespective of the noise connection.

With the configuration of Fig. 9 a subsidiary amplifier gain of 44 dB was required to yield a second-stage error cancellation loop balance. Because of overdrive considerations, the balance of the error sensor loop which drives the subsidiary amplifier was critical. A worst null figure was found of 38 dB, but we might expect even better performance with more fastidious equalization since such improved equalization is justified in light of the prior stabilization of the first stage. In contrast, such an attempt to improve error sensor loop balance in the first stage could not be justified in view of the relative softness of the main amplifier.

Accepting the 38-dB worst null figure, and accepting, further, a -1.5-dBm input necessary to drive the two-stage feed-forward system to its operating level, the 44-dB subsidiary amplifier gain in conjunction with the 10-dB loss through the input coupler and 0.3 dB of added loss in the second-stage time delay circuit implies a -8.5-dBm output level of the final second-stage upconverter due only to imbalance effects introduced by the first stage. This power far exceeds that required to handle first-stage intermodulation and, consequently, dominates the power capacity required for the upconverter.

In order to expedite the program we used, in the second stage of feed-forward, commercially available components which were marginal in their power handling ability. This necessitated the addition of a second pilot tone at 4110 MHz and a phase controller to offset overload-producing imbalances created by thermal effects in the second-stage, error-sensor-loop, delay line. These additions would probably not be needed in final design.

For completeness, Fig. 10 shows the detection and control system actually employed. In essence, operation is based on the principle that a

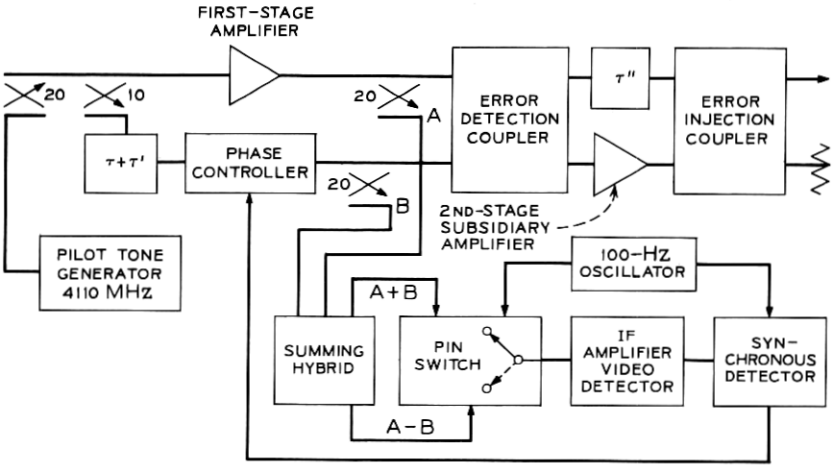

Fig. 10—Second-stage controller.

vector sum and a vector difference have the same magnitude only if the two component vectors are in perfect phase quadrature. This yields a phase sensing means for control feedback.

IV. EXPERIMENTAL RESULTS

A complete schematic of the full, two-stage system is given in Fig. 11, omitting third-loop correction features as irrelevant. Front and side photographic views of the system are given in Figs. 12 and 13.

As Fig. 11 shows, the experimental system leans heavily on ferrite loaded components for both adjustment and cautionary purposes. These would disappear, for the most part, substantially lowering losses appearing in an actual system. Conservative calculation of extraneous losses suggests that at least 2 dB of loss is recoverable in practice for a single stage over that achieved here, and twice that for a double correction stage.

4.1 *Saturation Curves*

Figure 14 shows gain as a function of output power for the uncorrected, first-stage corrected, and second-stage corrected microwave amplifier. The uncorrected amplifier shows very soft gain characteristics, with gain deviation observed as early as 12 dB below its 40-dBm saturation. The first and second corrected stages appear relatively identically shaped, but differ in their saturation power by the circuit losses. With

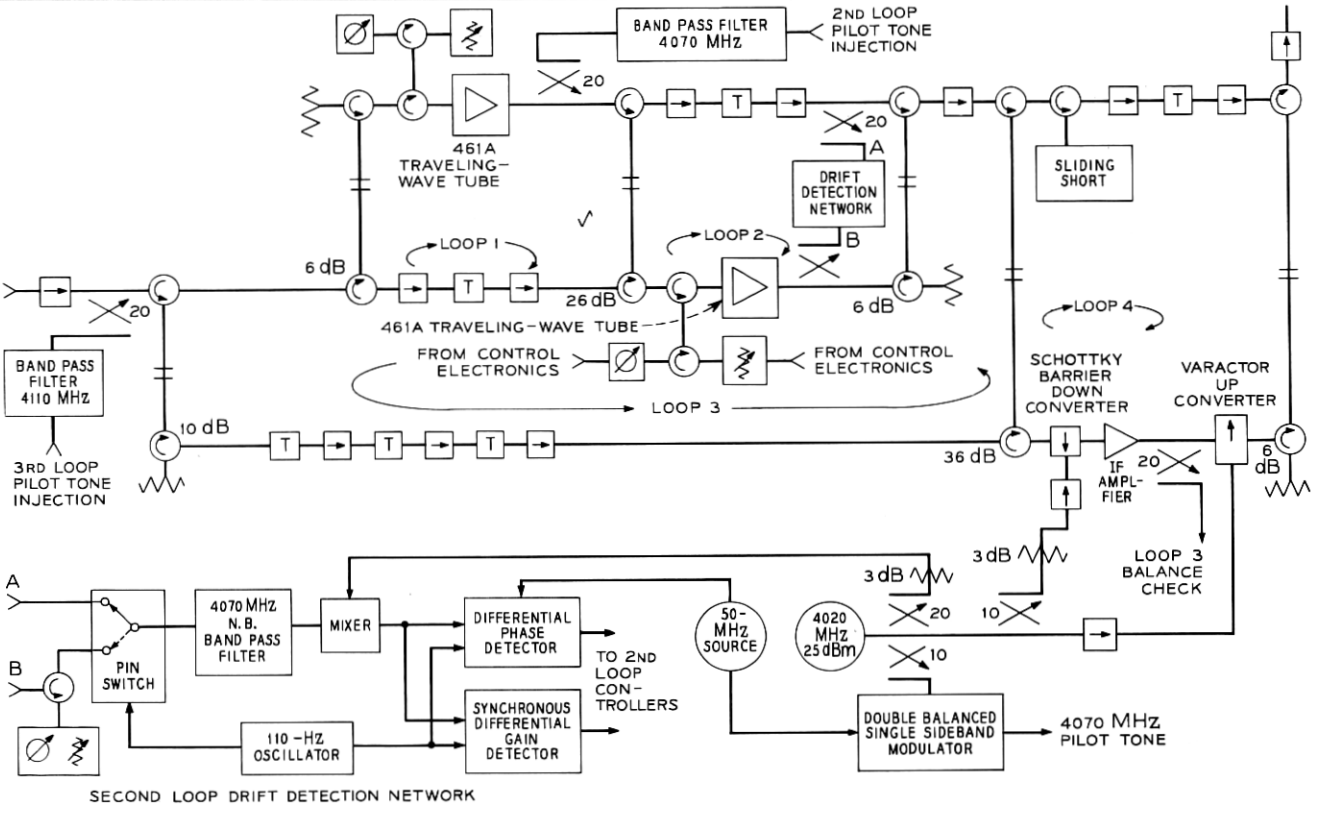

Fig. 11—Two-stage microwave feed-forward correction system.

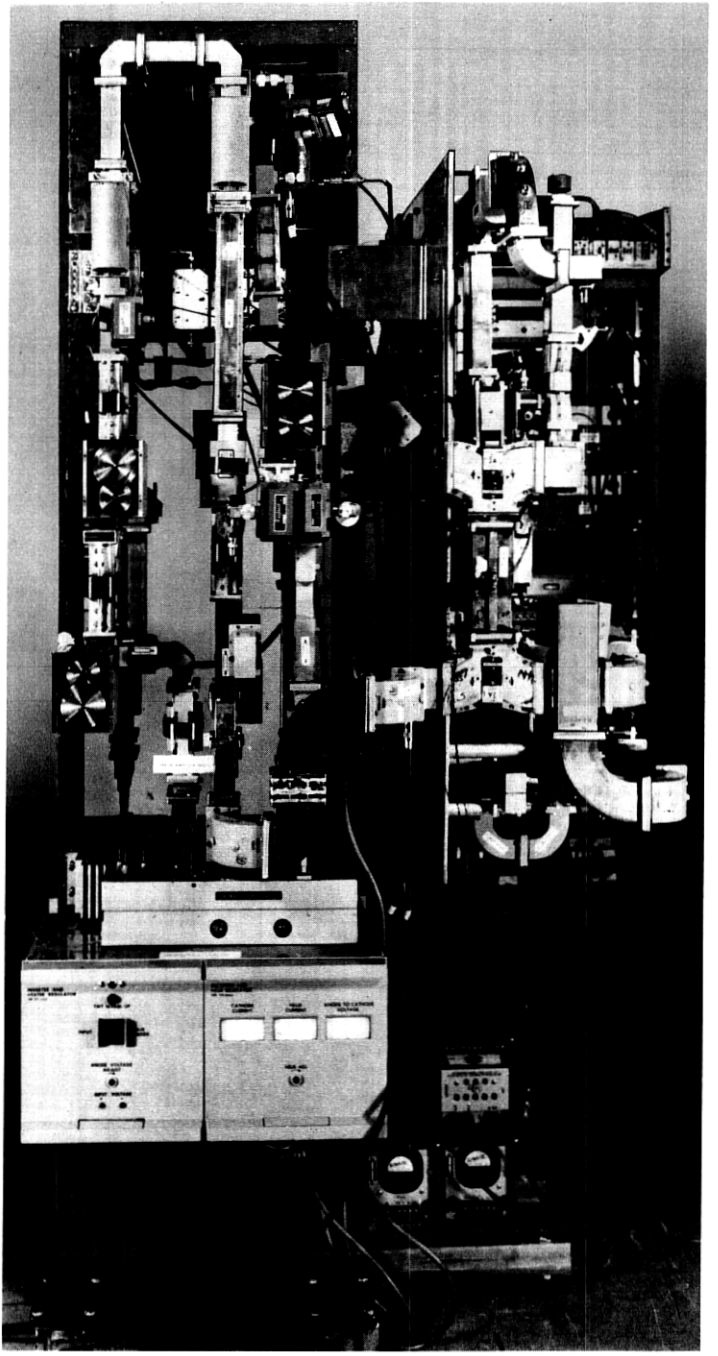

Fig. 12—Front view of system.

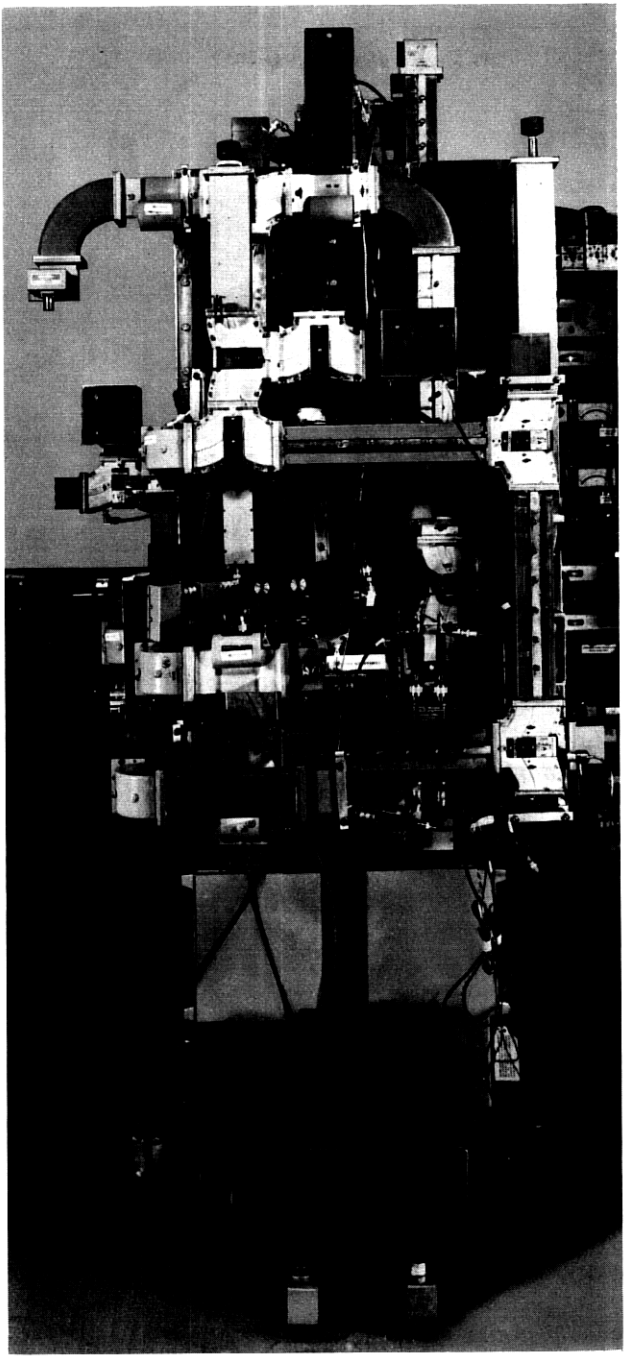

Fig. 13—Right-side view of system.

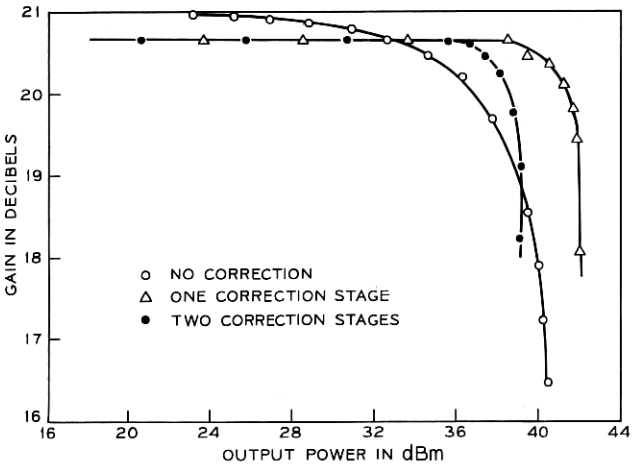

Fig. 14—Experimental gain characteristics.

first-stage correction, saturation occurs at about 42 dBm, while second stage correction reduces this to 39 dBm. Discounting extraneous losses of 2 dB per stage, these numbers would correspond in practice to 44 and 43 dBm, respectively. In contrast to the uncorrected amplifier, gain is a far flatter function in the corrected systems, showing the onset of gain deviation within only 3 dB of saturation.

Figure 15 shows corresponding phase characteristics. The phase curve of the uncorrected amplifier shows the same sort of softness as does the gain curve, while first- and second-stage correction yield a remarkable flattening. To within a phase variation of, perhaps, 1 degree peak to peak, there is no marked deviation from flatness until about 2 dB from saturation.

4.2 *Dump Port Power*

First-stage error cancellation injection is performed via a 6-dB four-port coupler. Three ports are occupied with main path transmission and error injection, while the fourth is resistively terminated to assure the match and directivity properties of the coupler.

A serious concern is expressed in Ref. 4 about the use of a four-port for this function since the resistive termination operates to absorb 1 dB of main path power for a 6-dB coupler. It is easily shown, however, that by choosing the reference phase and gain appropriately in the first-stage error sensor loop, a destructive interference occurs into that termination

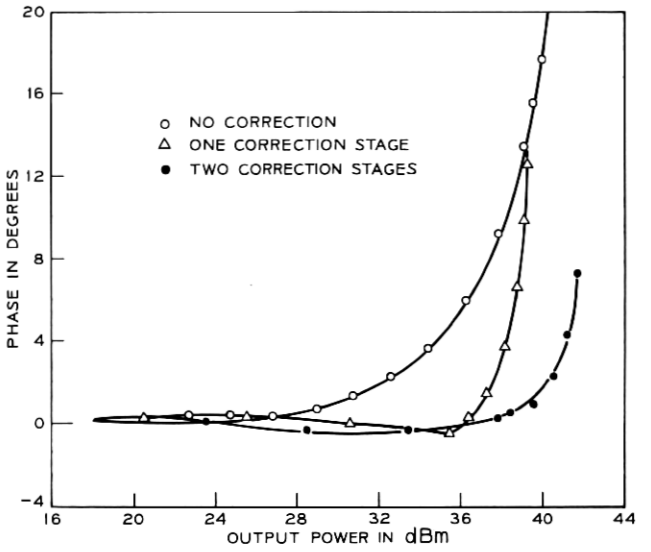

Fig. 15—Experimental phase characteristics.

of the wave portion coupled from the main amplifier and the portion transmitted from the error amplifier. Under this circumstance, with only small power entering the termination, most of the power lost by the main amplifier is recaptured and is further augmented by virtually all the power emitted by the subsidiary amplifier. We can, in principle, arrange this condition at some most critical operating point of the system, turning the injection coupler from a liability to an asset.

This process is made evident in Fig. 16 which shows dump-port power as a function of output power. At low levels, only small error power is generated and the dump power is dominated by main line coupling. This is evidenced by a linear dB for dB relationship. At 36 dBm output, however, the coupling into the termination is 9 dB below a linear coupling rate, representing a relatively minor system power loss with respect to the combined power emissions of both the main and subsidiary amplifiers.

4.3 *Intermodulation Results*

The reduction of intermodulation is a function of the various interferometer loop balances. The first- and second-stage error injection nulls measured minimally 42 and 38 dB, respectively, across the band suggesting, ideally, an 80-dB two-stage distortion correction capability,

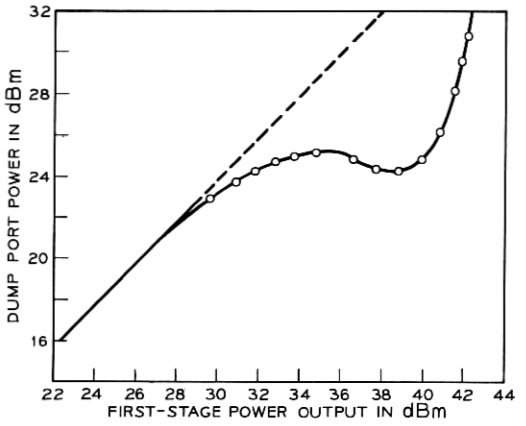

Fig. 16—First-stage dump port power.

disregarding losses added by the two stages. As measured, the error sensor null of the first stage exceeded 35 dB, which was ample to avoid observable distortion in the 461A TWT subsidiary amplifier. While the error sensor null of the second stage was 37 dB it proved only marginally adequate in avoiding saturation onset in the second-stage subsidiary amplifier. Estimation suggests, nevertheless, that greater than 50 dB distortion reduction was achieved with both correction stages operating.

The intermodulation tests were made with three tones, each driving the first-stage-corrected traveling-wave tube amplifier to a 22-dBm output. Taking actual losses into account, this corresponds to a 25-dBm/tone output of the uncorrected TWT. With the addition of the second stage, this output level was reduced by the additional loss to about 19 dBm/tone. Two of the tones were fixed at 4.080 and 4.100 GHz, respectively, while the third was adjusted to discrete positions across the 20-MHz band. To provide improved dynamic range of the intermodulation equipment a coherent main tone cancellation scheme was employed. The three input tones were sampled, individually processed, and reintroduced following the amplifier in a fashion to interfere destructively with the tones transmitted by the amplifier.

The intermodulation test set apparatus is depicted in Fig. 17. For simplicity of display while moving the variable tone signal a delay line was introduced in tandem with the combined cancellation signals to maintain a phase-tracked interference with the test amplifier. A minimum interference of 35 dB to the signal tones was obtained across the

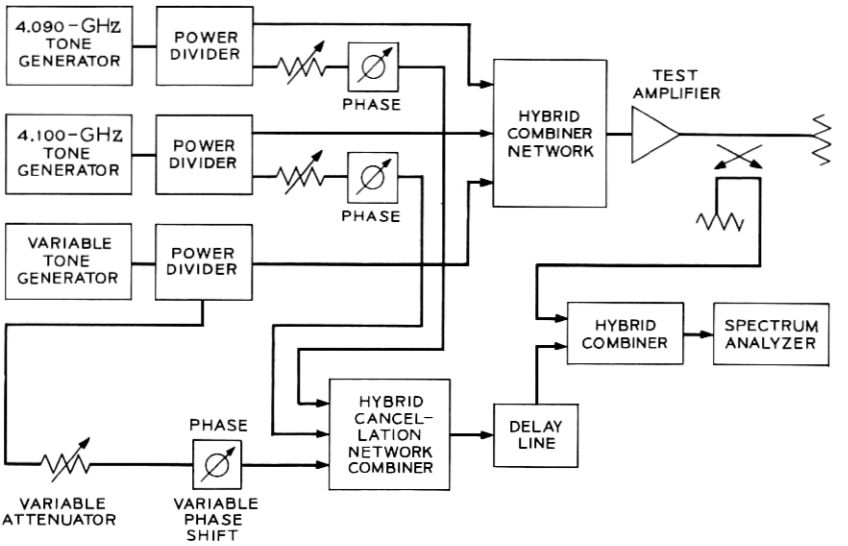

Fig. 17—Intermodulation test set.

4.080- to 4.100-GHz band with no observable interaction to the modulation tones.

Figure 18a shows the amplifier at what would normally be the second-stage output, but with both first and second correction stages disabled. The adjustable tone is set at 4.092 GHz and intermodulation products are observed ranging up to about −9 dBm. Considering the 6-dB loss sustained from the output of the main line TWT to the second-stage output, this corresponds to an intermodulation production of −3 dBm. This quantity is excellently consistent, at 25 dBm/tone excitation, with the −78-dB M3 measure given the 461A.

As we shall find in the tabulation to follow, one may identify products down to ninth order. The dominant term with which we are mostly concerned here is the third-order A + B − C product, given as the image with respect to band center of the adjustable tone. This product, shown at 4.088 GHz, has the −9-dBm value alluded to earlier. Visible in the figure are pilot tones at 4.070 and 4.110 GHz, respectively.

Figure 18b shows the effect of a single correction stage. The dominant third-order tone is reduced well beyond 40 dB, and all others in-band are rendered virtually invisible. We may observe that the 4.070-GHz pilot tone which lies well below band is reduced by 25 dB, showing that error degeneration is still somewhat effective at that frequency. The 4.110

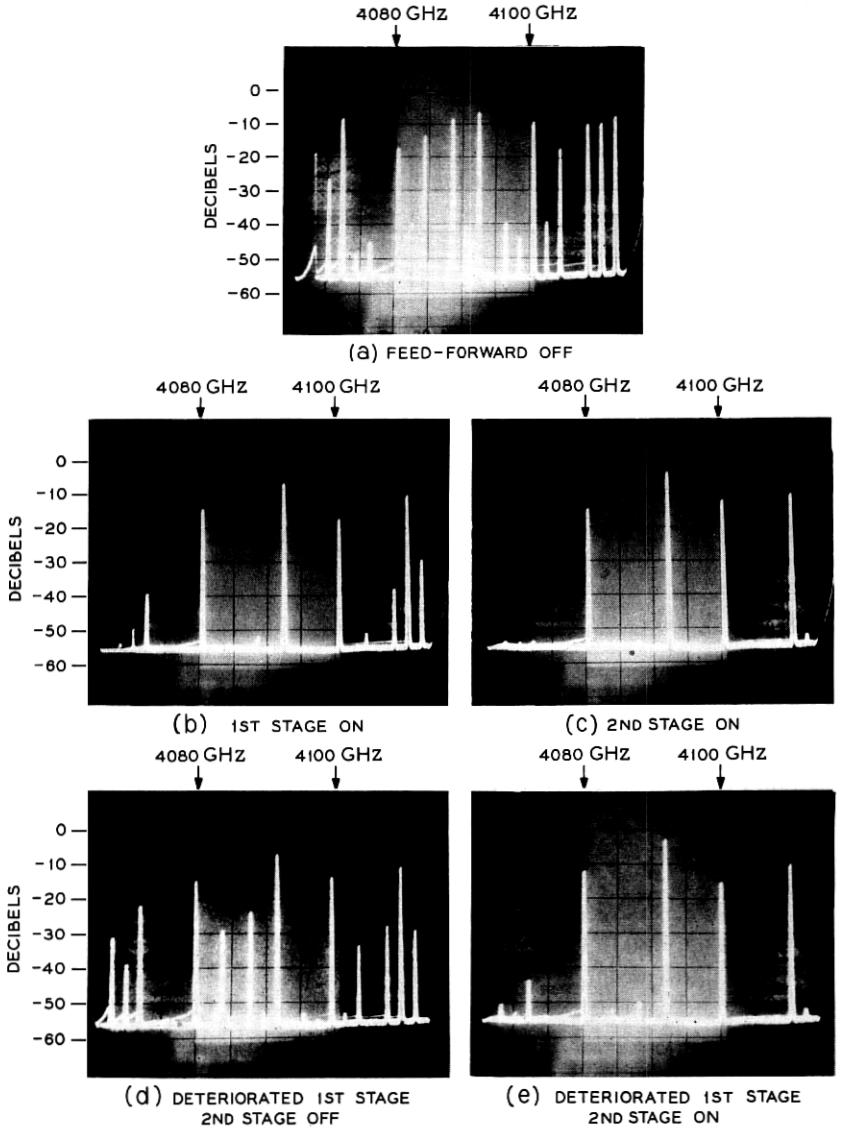

Fig. 18—Spectograms of modulation products.

tone, unlike that at 4.070, is not introduced in the fashion of simulating noise, but rather it enters the system as a spurious signal. It will be observed that it, like the signal tones, is unaffected by feed-forward correction.

Figure 18c, showing application of the second stage, reduces all intermodulation products into the base line. We observe that it wipes out the residue of the 4.070-GHz pilot, but it leaves some vestigial bumps at 4.088 and 4.085 which were visible with first-stage correction. The fact that the pilot was removed, and the bumps not, suggests that the second stage operates to remove previously generated products, but that it has generated new ones in the process. This corresponds with our concern over the weak upconverter stage.

To confirm this mode of second-stage operation, Fig. 18d shows the effect of fully disabling the second stage, but of only partially detuning the first-stage error injector loop. It resembles Fig. 18a but the intermodulation products are down by about 15 dB. Leaving the detuned first stage untouched, the second stage is reenergized, producing the result of Fig. 18e. We find concellation exceeding 30 dB but, again, the telltale bumps suggest a residual level corresponding to newly generated intermodulation products.

To give a more quantitative measure to the results shown on the various spectrograms, these same results were tabulated point by point in Table I on a Western Electric 39A measuring set. The vestigial bumps with second-stage correction, barely observable visually, cannot be found at all in the measuring set. Therefore, no second-stage observations appear. This level of unresolvability within the 39A corresponded to about a -55-lBm amplifier output level and, consequently, accounts for the general vacancy of entries with first-stage correction as well.

The tabulation corresponds to output differences of 3 dB between the uncorrected and corrected stages, and mirrors losses, for the most part, attributable to experimental implementation. A realistic difference in practice would be close to 1 dB, losing 5 dB in distortion reduction for third-order products over that obtained by directly differencing the last two columns of Table I. Extrapolating to a system in practice, the results with the adjustable tone at 4.092 GHz, for example, would show a first-stage correction of 37.7 dB, an M3 value of -116.2 dB, corresponding to a 28.8-dBm average power, and the peaking of a single 33.6-dBm tone.

From the first stage data it is observed that a reduction of greater than 40 dB occurs throughout with the first stage operating as opposed to its being disabled but remaining in position. This result is consistent

TABLE I—INTERMODULATION RESULTS

Adj. Freq.	Modulation Product Order	Produce Freq.	Uncorrected† (25 dBm Out)	1st Stage† (22 dBm Out)
4098	3	4082	−4.5 dBm	−47.5 dBm
		4096	−9.2	—
	5	4084	−34.5	—
		4094	−41.3	—
	7	4086	−41.5	—
		4092	−37.3	—
	9	4088	−34.5	—
		4090	−34.5	—
4096	3	4084	−3.5	−46
		4092	−8.2	—
	5	4088	−44.2	—
4092	3	4084	−9	—
		4088	−3.5	−46.2
	5	4096	−34.2	—
4089	3	4091	−5.1	−50.5
		4098	−14.4	—
	5	4082	—	—
		4087	−39.8	—
4086	3	4092	−12.9	—
		4094	−3.6	−50.5
	5	4088	−38.0	—
		4098	−44.5	—
4083	3	4086	−14.3	—
		4097	−5.4	−52
	5	4089	−45	—
		4094	−39	—

† The absence of datum indicates its unresolvability on the measuring equipment used and represents power < -54 dBm.

with the 42-dB minimum interferometer null of the error injector loop portion of the first stage. This correlation to measurement, although it could not be made with the second stage as well because of inadequate power capacity, is gratifying. First, it confirms the fundamental operations principles of feed-forward. Secondly, it demonstrates the sufficiency of a frequency swept interferometer null measurement and this is important in providing an intrinsically simple field procedure for setting up and maintaining a feed-forward microwave amplifier system.

V. COMMENTS AND SUMMARY

With first-stage correction, and at a 22-dBm power level per tone, with a three-tone excitation, all intermodulation products were reduced by the order of 40 dB or more over those of an uncorrected 461A traveling-wave tube amplifier. With second stage correction these products were unmeasurable with instruments available to us.

The use of feed-forward techniques in microwave applications suggests the need to review the precise nature and meaning of distortion measure in view of precipitous distortion increase with subsidiary amplifier saturation. Those specifications set for the present experiment might well have been met with a smaller first-stage subsidiary amplifier but recent, more rigid, specifications suggest ultimate use of the full power capacity of the 461A tube used.

Nowhere in the scope of the experiment was an attempt made to evaluate the economics of a higher performance single-stage versus an equally performing multistage correction system, with a lower quality of performance per stage. Nevertheless, the distortion reduction presently achievable with a single 461A TWT subsidiary amplifier correction stage is not too far from the objective of 47 dB sought. We feel this figure to be realistic with improved equalization, providing that the power supply is also improved in terms of the hum content that presently limits performance.

It is in the nature of the electronic art that a new device, initially viewed as a substitution for other devices which it overlaps, finds a niche quite apart from the one contemplated. The transistor, originally a substitute for the vacuum tube, proved amenable to a radical revamping of use, and shifted the very arts which employed it. Within this context, the new existence of a highly linear microwave amplifier suggests review by communication analysts as to the role of analog devices in this portion of the spectrum.

VI. ACKNOWLEDGMENTS

It is a pleasure to acknowledge a laboratory-wide support in this traveling-wave experiment, and I regret any slight to many not mentioned. Most notably, major responsibilities for system integration and operation rested with H. R. Beurrier and C. H. Bricker. Mr. Beurrier was responsible for first-stage operation, and designed and constructed the control circuitry. Mr. Bricker built both the second stage and the intermodulation measurements equipment.

A. J. Giger's initial studies established the levels of device linearity necessary in single sideband transmission. His comments were much valued during the course of the experiment.

Finally, I am indebted to W. E. Danielson for stimulating this project and to F. H. Blecher and E. D. Reed for their kind encouragement and support.

APPENDIX

Scattering Matrix Simplifications

The noise formulation in Section 2.2 is considerably simplified by the application of energy conservation and time reversibility relationships implicit in the couplers used. As stated in equations (4) and (5), and as a result of these relationships, a coupler scattering matrix,

$$S = \begin{bmatrix} 0 & 0 & S_{13} & S_{14} \\ 0 & 0 & S_{23} & S_{24} \\ S_{13} & S_{23} & 0 & 0 \\ S_{14} & S_{24} & 0 & 0 \end{bmatrix}, \tag{12}$$

must satisfy the unitary requirement,

$$\begin{bmatrix} 0 & 0 & S_{13}^* & S_{14}^* \\ 0 & 0 & S_{23}^* & S_{24}^* \\ S_{13}^* & S_{23}^* & 0 & 0 \\ S_{14}^* & S_{24}^* & 0 & 0 \end{bmatrix} \begin{bmatrix} 0 & 0 & S_{13} & S_{14} \\ 0 & 0 & S_{23} & S_{24} \\ S_{13} & S_{23} & 0 & 0 \\ S_{14} & S_{24} & 0 & 0 \end{bmatrix} = \begin{bmatrix} 1 & 0 & 0 & 0 \\ 0 & 1 & 0 & 0 \\ 0 & 0 & 1 & 0 \\ 0 & 0 & 0 & 1 \end{bmatrix}. \tag{13}$$

A series of relationships yielded by (13):

(*i*) $$| S_{13} |^2 + | S_{14} |^2 = 1,$$

(*ii*) $$| S_{13} |^2 + | S_{23} |^2 = 1,$$

(*iii*) $$| S_{23} |^2 + | S_{24} |^2 = 1.$$

From *i* and *ii*,

(*iv*) $$| S_{14} |^2 = | S_{23} |^2,$$

and, using *iii*,

(*v*) $$| S_{13} |^2 = | S_{24} |^2.$$

From the zero elements of the unit matrix we find:

(*vi*) $$S_{13}S_{14}^* + S_{23}S_{24}^* = 0,$$

(*vii*) $$S_{13}S_{23}^* + S_{14}S_{24}^* = 0.$$

We apply these relationships first to find a simplification for $\mathcal{G}$. From (1),

$$G_1 = -\frac{S_{24}^{(1)} S_{24}^{(2)}}{S_{23}^{(1)} S_{14}^{(2)}}. \tag{14}$$

Using this result in (3) we find

$$\mathcal{G} = \frac{S_{24}^{(1)} S_{13}^{(3)}}{S_{14}^{(2)}} (-S_{13}^{(2)} S_{24}^{(2)} + S_{14}^{(2)} S_{23}^{(2)}). \tag{15}$$

Recognizing from *vi* that

$$S_{13}^{(2)} = -\frac{S_{23}^{(2)} S_{24}^{(2)*}}{S_{14}^{(2)*}}, \tag{16}$$

yields

$$\mathcal{G} = \frac{S_{24}^{(1)} S_{13}^{(3)} S_{23}^{(2)}}{|\, S_{14}^{(2)} \,|^2} (|\, S_{24}^{(2)} \,|^2 + |\, S_{14}^{(2)} \,|^2). \tag{17}$$

Since the portion in parenthesis is unity by virtue of the unitary relations, and using the equality of *iv*, we obtain the result given in (6); namely,

$$\mathcal{G} = \frac{S_{24}^{(1)} S_{13}^{(3)}}{S_{23}^{(2)*}}. \tag{18}$$

Simplification of the noise formulation follows easily along the same lines. Equation (7) yields

$$\epsilon = U_o[S_{14}^{(1)} S_{24}^{(2)} G_2 S_{23}^{(3)} + S_{14}^{(1)} S_{23}^{(2)} S_{13}^{(3)}] + U_2 G_2 S_{23}^{(3)}. \tag{19}$$

From (2),

$$G_2 = -\frac{S_{13}^{(2)} S_{13}^{(3)}}{S_{14}^{(2)} S_{23}^{(3)}}. \tag{20}$$

Combining, we find

$$\epsilon = \frac{S_{13}^{(2)} S_{13}^{(3)}}{S_{14}^{(2)}} \left[U_o \left(- S_{24}^{(2)} + \frac{S_{14}^{(2)} S_{23}^{(2)}}{S_{13}^{(2)}} \right) S_{14}^{(1)} - U_2 \right]. \tag{21}$$

From *vi*,

$$\frac{S_{23}^{(2)}}{S_{13}^{(2)}} = -\frac{S_{14}^{(2)*}}{S_{24}^{(2)*}},$$

so that

$$\epsilon = -\frac{S_{13}^{(2)} S_{13}^{(3)}}{S_{14}^{(2)} S_{24}^{(2)*}} [U_o S_{14}^{(1)} + U_2 S_{24}^{(2)*}]. \tag{22}$$

Since, by *vii*, $S_{14}^{(2)} S_{24}^{(2)*} = -S_{13}^{(2)} S_{23}^{(2)*}$, we find

$$\epsilon = \frac{S_{13}^{(3)}}{S_{23}^{(2)*}} \mid U_o S_{14}^{(1)} + U_2 S_{24}^{(2)*} \mid , \tag{23}$$

in agreement with (8).

The noise, normalized by the gain to yield an amplifier noise temperature, is found from combining the results of (18) and (23). We have

$$\frac{\epsilon}{\mathcal{G}} = \frac{U_o S_{14}^{(1)} + U_2 S_{24}^{(2)*}}{S_{24}^{(1)}}. \tag{24}$$

The autocorrelation of the above yields

$$\frac{\mid \overline{\epsilon^2} \mid}{\mid \mathcal{G}^2 \mid} = \frac{\mid S_{14}^{(1)} \mid^2 + T_2 \mid S_{24}^{(2)} \mid^2}{\mid S_{24}^{(1)} \mid^2}, \tag{25}$$

which agrees with (9) to within the recognition that $\mid S_{24} \mid^2 = \mid S_{13} \mid^2$.

REFERENCES

1. Black, H. S., U. S. Patent 1, 686, 792, issued October 9, 1929.
2. Bode, H. W., Proceedings of the Symposium on "Active Networks and Feedback Systems," Vol. X, Polytech Press of the Polytechnic Institute of Brooklyn, April 1960, pp. 1–17.
3. McMillan, B., U. S. Patent 2, 748, 201, issued May 29, 1956.
4. Seidel, H., Beurrier, H. R., and Friedman, A. N., "Error-Controlled High Power Linear Amplifiers at VHF," B.S.T.J., *47*, No. 5 (May–June 1968), pp. 651–722.
5. Seidel, H., "A Feedforward Experiment Applied to an L-4 Carrier System Amplifier," IEEE Trans. Commun. Tech., *COM-19*, No. 3 (June 1971), pp. 320–325.
6. Giger, A. J., private communication.
7. Hensel, W. G., and Sheets, L. L., individual private communications.
8. Members of Technical Staff, Bell Telephone Laboratories, *Transmission Systems for Communications*, Fourth Edition, February 1970, p. 252.
9. Brillouin, L., *Science and Information Theory*, New York: Academic Press, 1956, p. 153.
10. Dicke, R. H., Beringer, R., Kyhl, R. L., and Vane, A. B., Phys. Rev., *70*, 1946, p. 340.